Positive Identification of UV-Generated, Non-Hydrogen-Bonded Isomers of *o*-Hydroxybenzaldehyde and *o*-Hydroxyacetophenone

Leszek Lapinski,[†] Hanna Rostkowska,[†] Igor Reva,[‡] Rui Fausto,[‡] and Maciej J. Nowak*,[†]

Institute of Physics, Polish Academy of Sciences, Al. Lotnikow 32/46, 02-668 Warsaw, Poland, and Department of Chemistry, University of Coimbra, 3004-535 Coimbra, Portugal

Received: January 14, 2010

Non-hydrogen-bonded isomers were photogenerated by UV ($\lambda > 335$ nm) irradiation of *o*-hydroxybenzaldehyde (salicylaldehyde) and *o*-hydroxyacetophenone monomers isolated in low-temperature Ar matrixes. These photoisomerizations were found to be photoreversible. Upon shorter wavelength ($\lambda > 235$ nm or $\lambda > 270$ nm) UV irradiation, the initial forms of the compounds (with intramolecular hydrogen bonds) were partially repopulated. The structures of the photogenerated non-hydrogen-bonded isomers of both compounds were positively identified by comparison of their IR spectra with the spectra theoretically calculated [at the DFT(B3LYP)/6-311++G(2d,p) level] for all possible non-hydrogen-bonded isomers of the studied compounds. The experimental IR spectra of the photoproducts generated from *o*-hydroxybenzaldehyde and *o*-hydroxyacetophenone are very well reproduced only by the theoretical spectra predicted for the isomers with both OH and formyl (or acetyl) groups rotated by 180°, with respect to the initial, most stable hydrogen-bonded conformer. Excellent agreement between experiment and theoretical prediction provides a basis for a very reliable identification of the photoproduced isomers of *o*-hydroxybenzaldehyde and *o*-hydroxyacetophenone.

Introduction

The phenomenon of excited-state intramolecular proton transfer (ESIPT) has fascinated scientists already for several decades.[1,2] The ESIPT process is one of the most extensively and thoroughly studied photochemical reactions.[3] Application of modern techniques,[4−7] with enhanced time resolution, revealed that during this photoprocess proton is transferred extremely fast, within 40−60 fs. The unique properties of molecules exhibiting ESIPT process were employed for practical purposes, such as polymer photostabilization,[8−10] stimulated light emission in four-level lasers and data storage.[11−14]

o-Hydroxybenzaldehyde (OHBA, salicylaldehyde; see Chart 1) is the smallest aromatic molecule displaying ESIPT. Although proton transfer in OHBA is completed extremely fast (in less than 100 fs), the molecule is known to undergo another, competing UV-induced transformation. Gebicki and Krantz[15] were the first to report photogeneration of a non-hydrogen-bonded isomer of OHBA stabilized in a low-temperature Ar matrix. However, they were not able to determine which of the possible non-hydrogen-bonded structures (presented in Chart 2) was actually photoproduced. More extended study on this issue was carried out by Morgan et al.[16] By comparison of the IR, UV, and luminescence spectra of OHBA photoisomer with the spectra of several model compounds, these authors came to the conclusion that the **NPT3** form (see Chart 2) should be the most plausible structure of the non-hydrogen-bonded photoproduct. However, very recently, Migani et al.[17] carried out extended CASSCF and CASPT2 scans of the potential energy surfaces of the S_1 and S_0 states of OHBA. The authors claimed to have obtained a complete picture of the excited- and ground-state potential energy surfaces. The computational results

CHART 1: Structures of Most Stable, Hydrogen-Bonded (HB) Isomers of *o*-Hydroxybenzaldehyde (OHBA) and *o*-Hydroxyacetophenone (OHAP)

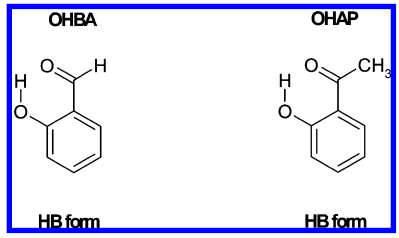

suggested that the non-hydrogen-bonded photoproduct of OHBA should have **PT2** or **PT3** structure (Chart 2), resulting from proton transfer to the formyl group and subsequent rotation of the HCOH moiety. The very recent experimental study,[18] on the photochemical behavior of 7-hydroxy-4-methylquinoline-8-carbaldehyde (a molecule bearing an OHBA subunit), demonstrated that proton transfer followed by rotation of the formyl group can indeed occur upon UV irradiation of OHBA analogues.

The theoretical calculations of Migani et al.[17] suggest also the possibility of UV-induced generation of another non-hydrogen-bonded isomer of OHBA, with an oxetene structure (**OXET**, Chart 2). A similar oxetene form was predicted by Sobolewski and Domcke[19] as one of the expected photoproducts of salicylic acid.

For *o*-hydroxyacetophenone (OHAP, see Chart 1), photogeneration of a non-hydrogen-bonded isomer was first claimed to be impossible.[15] Several years later, such an isomer was photoproduced,[20] though only upon extremely long irradiation (10 h with 6 mW laser at 320 nm, or 5 h with 1000 W Xe/Hg lamp) of OHAP isolated in Xe or SF_6 low-temperature matrixes. Matrix-cage hindrance to the rotation of the more voluminous acetyl group was thought to be the reason for difficulties in photoisomerization of OHAP in argon matrixes. No detailed

* To whom correspondence should be addressed. E-mail: mjnow@ifpan.edu.pl.
[†] Polish Academy of Sciences.
[‡] University of Coimbra.

10.1021/jp1003775
Published on Web 04/08/2010

CHART 2: Structures of Non-Hydrogen-Bonded Isomers of OHBA and OHAP

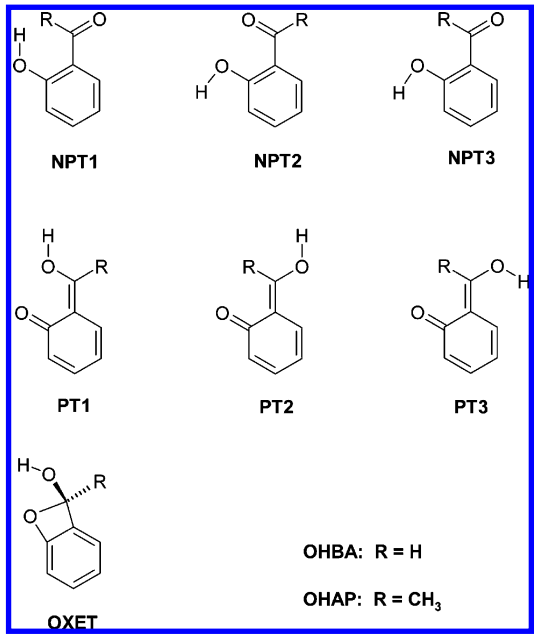

analysis of the structure of the obtained non-hydrogen-bonded form of OHAP has been reported.

In the present work, we studied the photoisomerization reactions of OHBA and OHAP molecules isolated in low-temperature Ar matrixes. The photogenerated non-hydrogen-bonded isomers of these compounds were identified by comparison of their experimental FTIR spectra with the spectra calculated for all possible candidate structures. For OHBA as well as for OHAP, a very good agreement between the theoretically predicted spectrum and the experimental spectrum of the photoproduct was found only for one of the candidate structures, providing a strong evidence of the correctness of the photoproduct structure identification.

Experimental Section

o-Hydroxybenzaldehyde and *o*-hydroxyacetophenone used in the present study were supplied by Aldrich (both with purity >99%). The compound to be studied was placed in a glass tube connected to the vacuum chamber of a cryostat through a regulating valve with shut-off possibility. Prior to a matrix experiment, the vapors over the compound were evacuated several times at room temperature. This approach enabled removal of possible volatile impurities, allowing an additional purification. For both compounds, the saturated vapor pressure over a sample kept at 0 °C was appropriate for deposition of a matrix. The vapors of *o*-hydroxybenzaldehyde or of *o*-hydroxyacetophenone were deposited, together with a large excess of argon, on a CsI window cooled to 12 K. The argon matrix gas was of spectral purity (N6.0), as supplied by Air Liquide. The IR spectra were recorded in the 4000−400 cm^{-1} range, with 0.5 cm^{-1} resolution, using a Thermo Nicolet 670 FTIR spectrometer equipped with a KBr beam splitter and DTGS detector. Intensities of the IR absorption bands were measured by numerical integration. Matrixes were irradiated with light from 200 W high-pressure mercury or xenon−mercury lamp fitted with a water filter and an appropriate cutoff filter. To study the dependence of the investigated photoprocess on the wavelength of the applied UV light, the WG335, UG11, or UG5 (Schott) cutoff filters (transmitting light with $\lambda > 335$ nm, $\lambda > 270$ nm, or $\lambda > 235$ nm, respectively) were used. In some experiments, matrixes were irradiated with frequency-doubled light of the signal beam emitted by the Quanta-Ray MOPO-SL pulsed (10 ns) optical parametric oscillator (fwhm ∼0.2 cm^{-1}, repetition rate 10 Hz, pulse energy ∼1 mJ at 250 nm) pumped with a pulsed Nd:YAG laser.

Computational Section

Geometries of the OHBA and OHAP isomers (presented in Charts 1 and 2) were fully optimized using the density functional method DFT(B3LYP) with the Becke's three-parameter exchange functional[21] and the Lee, Yang, Parr correlation functional.[22] The somewhat overcrowded **NPT1** structure of OHAP, was found to be a minimum on the DFT-calculated ground-state potential energy surface, separated from the minimum of **NPT3** form by a barrier as high as 19 kJ mol^{-1} (see Figure S1 in the Supporting Information). The geometry optimization performed for **NPT1** isomer of OHAP converged to a structure with C_s symmetry.

At the optimized geometries of all OHBA and OHAP isomers, harmonic vibrational frequencies and IR intensities were calculated using the same DFT(B3LYP) level of theory. All the calculations were performed with the Gaussian 03 program[23] using the standard 6-311++G(2d,p) basis set. To correct for the systematic shortcomings of the applied methodology (mainly for anharmonicity), the predicted vibrational wavenumbers were scaled down by a single factor of 0.98. For the most stable **HB** forms as well as for **NPT3** forms, the theoretical normal modes

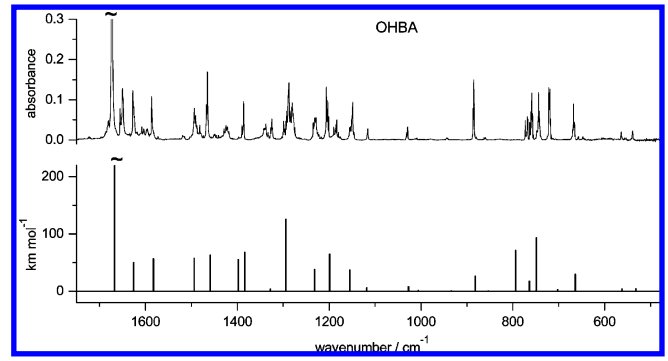

Figure 1. Infrared spectrum of OHBA monomers isolated in an Ar matrix (12 K), compared with the spectrum calculated [at the DFT(B3LYP)/6-311++G(2d,p) level] for the most stable, hydrogen-bonded form **HB** of the compound. Theoretical wavenumbers were scaled by 0.98. Very high intensity of the ν C═O band was truncated in the experimental and in the theoretical spectrum.

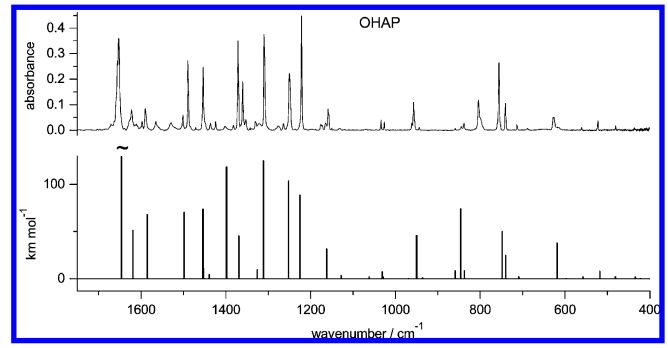

Figure 2. Infrared spectrum of OHAP monomers isolated in an Ar matrix (12 K), compared with the spectrum calculated [at the DFT(B3LYP)/6-311++G(2d,p) level] for the most stable, hydrogen-bonded form **HB** of the compound. Theoretical wavenumbers were scaled by 0.98. Very high intensity of the theoretical ν C═O band was truncated.

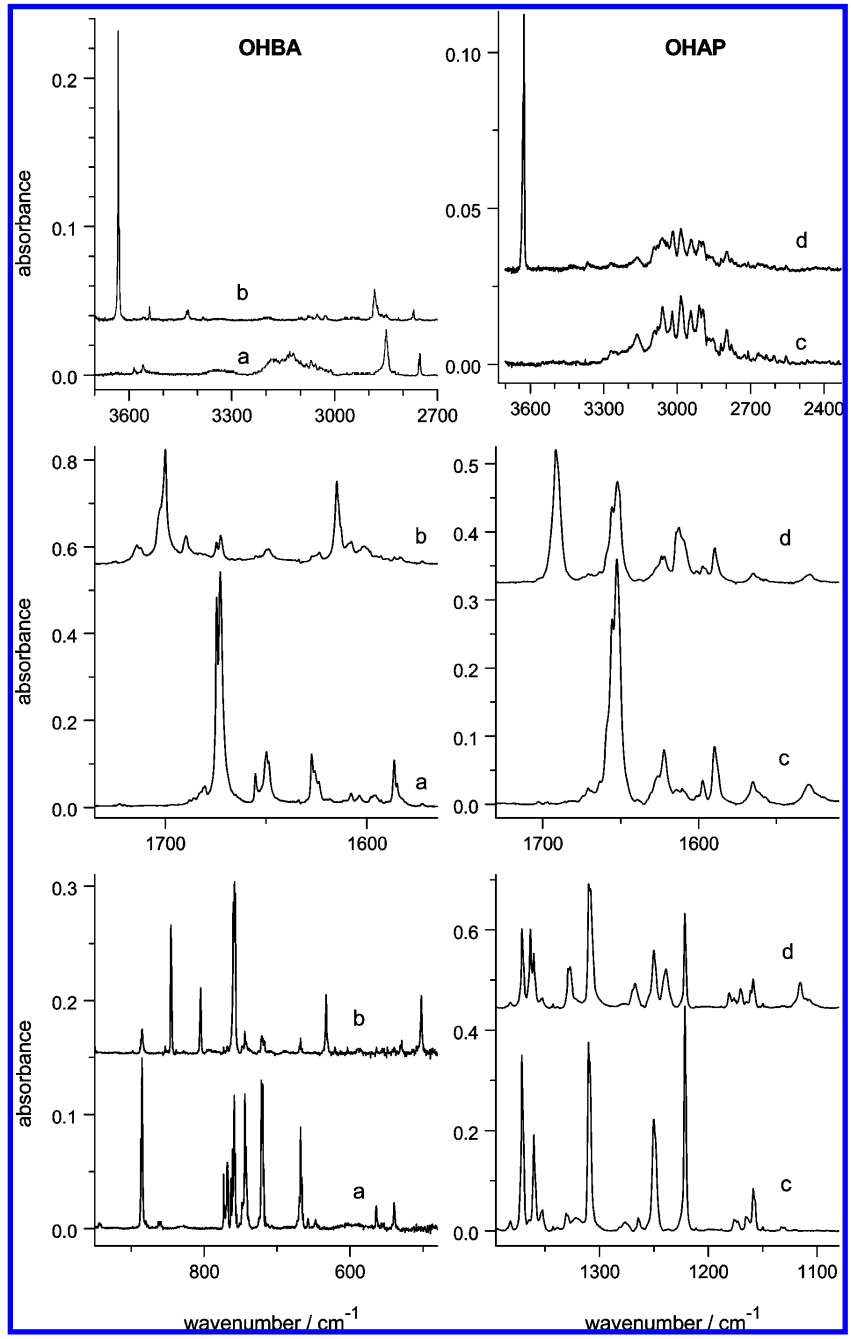

Figure 3. Changes observed in the infrared spectra of OHBA and OHAP monomers isolated in Ar matrixes (12 K) upon irradiation with UV light: (a) spectrum of OHBA recorded before irradiation; (b) spectrum of OHBA recorded after 1 h of UV ($\lambda > 335$ nm) irradiation; (c) spectrum of OHAP recorded before irradiation; (d) spectrum of OHAP recorded after 5 $^1/_2$ h of UV ($\lambda > 335$ nm) irradiation.

were analyzed by carrying out the potential energy distribution (PED) calculations.[24,25] The Cartesian force constants obtained from the DFT(B3LYP) calculations were transformed to the molecule-fixed internal coordinates system defined following the recommendations of Pulay et al.[26] The chosen coordinates are listed in Table S1 (in the Supporting Information). Potential energy distribution matrices have been calculated, and the elements of these matrices greater than 10% are given in Tables S2−S5 (in the Supporting Information).

Results and Discussion

Infrared Spectra of OHBA and OHAP Monomers. The isomers of OHBA and of OHAP with intramolecular hydrogen bonds closing a six-membered ring (**HB** forms shown in Chart 1) are by far the most stable forms of these compounds. According to the DFT(B3LYP)/6-311++G(2d,p) predictions, the energies of the non-hydrogen-bonded isomers of these compounds (presented in Chart 2) should be higher by more than 30 kJ mol^{-1} (see Tables S6 and S7 in the Supporting Information). Such a substantial difference in energy indicates that only forms with intramolecular hydrogen-bond (**HB**) should be populated in the gas phase and, as a consequence, trapped in low-temperature matrixes. The infrared spectra of monomeric OHBA and OHAP isolated in Ar matrixes are presented in Figures 1 and 2, respectively. No bands appear in these spectra in the region 3650−3500 cm^{-1}, characteristic of vibrations of OH groups not involved in hydrogen bonding (see Figure 3a,c). IR bands due to "free"

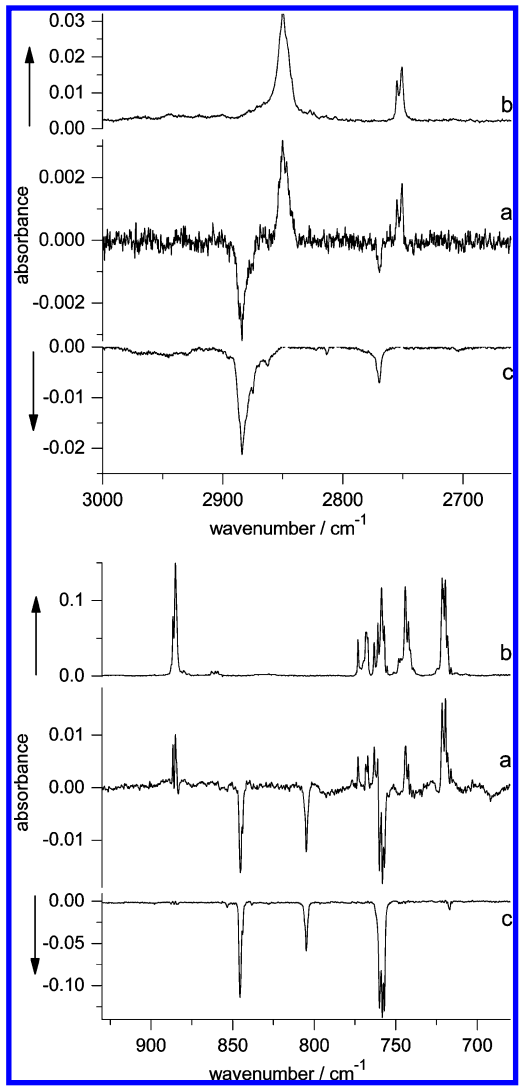

Figure 4. Partial photoreversibility of OHBA photoisomerization: (a) difference spectrum = (the spectrum recorded after 30 min of UV (λ > 235 nm) irradiation following 1 h of UV (λ > 335 nm) irradiation) minus (the spectrum recorded after 1 h of UV (λ > 335 nm) irradiation); (b) infrared spectrum of OHBA monomers isolated in an Ar matrix at 12 K; (c) extracted spectrum of the photoproduct generated upon UV (λ > 335 nm) irradiation, shown in reversed intensity scale.

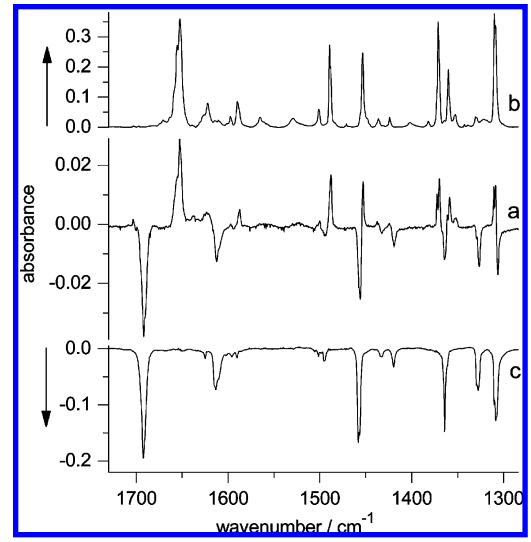

Figure 5. Partial photoreversibility of OHAP photoisomerization: (a) difference spectrum = (the spectrum recorded after 30 min of UV (λ > 270 nm) irradiation following 5 $^1/_2$ h of UV (λ > 335 nm) irradiation) minus (the spectrum recorded after 5 $^1/_2$ h of UV (λ > 335 nm) irradiation); (b) infrared spectrum of OHBA monomers isolated in an Ar matrix at 12 K; (c) extracted spectrum of the photoproduct generated upon UV (λ > 335 nm) irradiation, shown in reversed intensity scale.

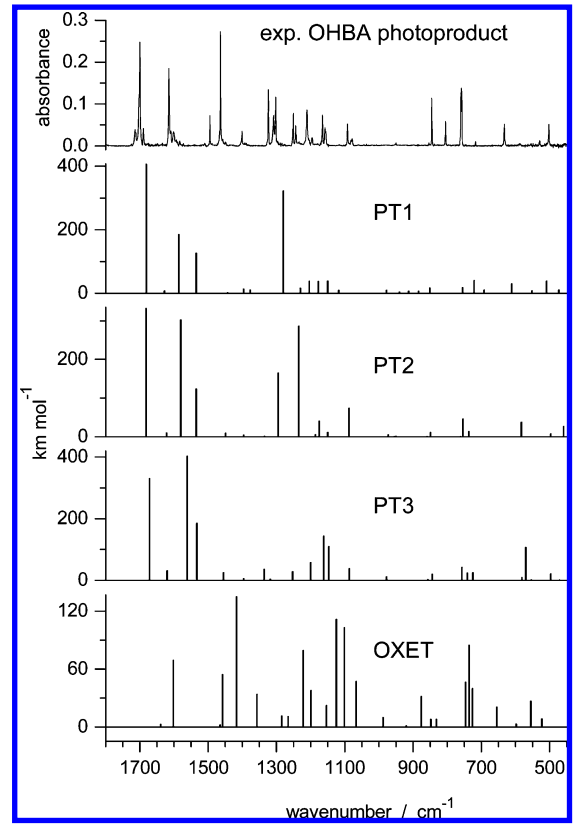

Figure 6. Comparison of the experimental IR spectrum of a photoproduct generated upon UV (λ > 335 nm) irradiation of OHBA with the spectra theoretically predicted for isomers **PT1**, **PT2**, **PT3**, and **OXET** of the compound. The theoretical spectra were calculated at the DFT(B3LYP)/6-311++G(2d,p) level. Theoretical wavenumbers were scaled by 0.98.

OH groups should appear in the spectra of all isomers of OHBA and OHAP shown in Chart 2, because in these structures OH groups are not involved in hydrogen bonding.

In the spectrum of OHBA monomers in an Ar matrix, a very broad absorption was observed at 3200−3000 cm^{-1} (see Figure 3a). This band of very large integrated intensity should be assigned to the stretching vibrations of the OH group (ν OH) involved in the intramolecular hydrogen bond with the formyl (OHBA) moiety. The analogous band was not observed clearly in the IR spectrum of OHAP, since for this compound the bands originating from CH stretching vibrations obscure the 3200−3000 cm^{-1} spectral range (Figure 3c). Moreover, if the intramolecular hydrogen bonding in OHAP is stronger than in the OHBA molecule, then the ν OH band of OHAP should be even more broadened and shifted to lower frequencies. There are several reasons to believe that the intramolecular hydrogen bond in OHAP is stronger than in OHBA. First, the calculated energy difference between **NPT2** and **HB** forms of OHAP (53 kJ mol^{-1}) is larger than the energy difference between the analogous forms of OHBA (44 kJ mol^{-1}); see Tables S6 and S7 in the Supporting Information. Second, the calculated frequency of the ν OH band in **HB** form of OHAP (3221 cm^{-1}) is lower than that predicted for the **HB** form of OHBA (3311 cm^{-1}). Finally, the experimental and theoretically predicted

position of the band due to the torsional vibration of OH (τ OH) is higher for OHAP (experimental, 804 cm^{-1}; calculated, 846 cm^{-1}) than for OHBA (experimental, 722, 720 cm^{-1}; calculated, 794 cm^{-1}); see Tables S3 and S2. Shifts of ν OH frequency toward lower values as well as shifts of τ OH frequency toward higher values provide a measure of the hydrogen bond strength.[27] For phenol monomers isolated in an Ar matrix,[28] where the OH group attached to the aromatic ring is not involved in hydrogen bonding, the ν OH band was observed at 3635 cm^{-1}, whereas in the spectrum of gaseous phenol[29] the τ OH band was found at 309.2 cm^{-1}. Another manifestation of the intramolecular hydrogen-bonding interaction in OHBA and OHAP may be observed for the bands due to the stretching vibration of the C═O group (ν C═O). The spectral position of the ν C═O bands is evidently shifted to lower wavenumbers (OHBA, 1673 cm^{-1}; OHAP, 1652 cm^{-1}), with respect to the corresponding bands of benzaldehyde (1717 cm^{-1}, Ar)[30] and acetophenone (1700 cm^{-1}, Ar)[31] monomers isolated in Ar matrixes. In the latter molecules, there is no intramolecular H-bond interaction.

The experimental IR spectra of OHBA and OHAP monomers isolated in Ar matrixes are compared in Figures 1 and 2 with the spectra of **HB** isomers of these compounds calculated at the DFT(B3LYP)/6-311++G(2d,p) level. Although the anharmonicity of the vibrations of the groups directly involved in the hydrogen bonding is significant, the correspondence between the experimental spectra and the theoretical spectra calculated within the harmonic approximation is quite good. This allowed assignment of the IR bands in the spectra of both compounds (the assignment is presented in Tables S2 and S3 in the Supporting Information).

UV-Induced Isomerizations of OHBA and OHAP. Irradiation of matrix-isolated OHBA with UV ($\lambda > 335$ nm) light led to significant changes in the IR spectra. Upon 1 h of irradiation the intensities of the IR bands in the initial spectrum decreased by 90% (see Figure 3b) and a new spectrum of the photoproduced form appeared. More prolonged irradiation did not induce any further spectral changes. Subsequent irradiation of the matrix with UV ($\lambda > 235$ nm) light resulted in partial repopulation of the initial hydrogen-bonded form of OHBA (see Figure 4).

In the IR spectrum of the photoproduct, the most striking feature was the appearance of a sharp and intense band in the high frequency region: at 3631 cm^{-1}, with a shoulder at 3629 cm^{-1}. This band should be assigned to the stretching vibration of a non-hydrogen-bonded OH group. For phenol monomers isolated in an Ar matrix,[28] the ν OH band was found at a very similar position (3635 cm^{-1}). In the spectral region characteristic of the ν C═O vibration, a new band appeared at 1700 cm^{-1}, i.e., at a wavenumber higher by 27 cm^{-1} with respect to the wavenumber of the ν C═O band observed in the initial spectrum. This finding also indicates the lack of intramolecular hydrogen bonding in the structure of the photoproduct.

The spectral changes occurring upon UV irradiation of OHAP were analogous to those observed for OHBA. Exposure of monomers of OHAP to UV ($\lambda > 335$ nm) light induced, though noticeably slower than for OHBA, a transformation of the initial form of the compound into a photoproduct. After 5 $^1/_2$ h of irradiation, 60% of the initial **HB** form of OHAP was consumed in the photoreaction and a photostationary state was achieved (Figure 3d). In the spectrum of the photoproduct new bands due to ν OH and ν C═O vibrations were found at 3625 cm^{-1} (with a shoulder at 3629 cm^{-1}) and 1692 cm^{-1}, respectively. These observations suggest that non-hydrogen-bonded product is photogenerated also in the case of OHAP. Subsequent irradiation with UV ($\lambda > 270$ nm) light led to a partial recovery of the initially deposited **HB** isomer of OHAP (Figure 5). Upon this shorter-wavelength irradiation a new photostationary state was attained.

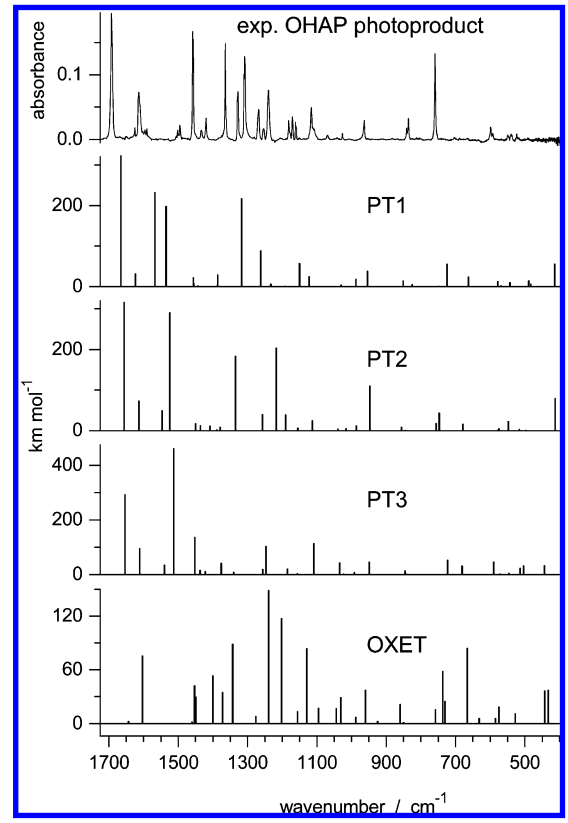

Figure 7. Comparison of the experimental IR spectrum of a photoproduct generated upon UV ($\lambda > 335$ nm) irradiation of OHAP with the spectra theoretically predicted for isomers **PT1**, **PT2**, **PT3**, and **OXET** of the compound. The theoretical spectra were calculated at the DFT(B3LYP)/6-311++G(2d,p) level. Theoretical wavenumbers were scaled by 0.98.

Identification of UV-Generated Non-Hydrogen Bonded Isomers of OHBA and OHAP. The non-hydrogen-bonded isomers of OHBA and of OHAP can be divided into three categories: (i) forms **NPT1**, **NPT2**, **NPT3**, obtained from the most stable structure of a compound by rotation of hydroxyl and formyl (or acetyl) groups, but without proton transfer (**NPT** stands for no proton transfer); (ii) forms **PT1**, **PT2**, **PT3**, obtained by proton transfer followed by rotation of the R−C−OH group as a whole and hydroxyl group within it; (iii) oxetene forms **OXET** (see Chart 2).

The infrared spectra of all non-hydrogen-bonded isomers of OHBA and OHAP were theoretically predicted at the DFT(B3LYP)/6-311++G(2d,p) level. Comparison of the experimental spectra of UV-generated forms of OHBA and OHAP with the IR spectra calculated for the **PT1**, **PT2**, **PT3** isomers of the compounds (presented in Figures 6 and 7) clearly reveals that the theoretical spectra calculated for the **PT** structures, with a proton transferred to the formyl (or acetyl) group, do not agree with the experimental spectra. No strong anharmonic effects should be expected for these non-hydrogen-bonded structures. Hence, if the structure was correct, the experimental spectra should be very well reproduced by theoretical simulations. The correspondence between the experimental spectra of the photoproduced OHBA and OHAP isomers and the spectra calculated for the respective oxetene (**OXET**) forms is dramatically bad (see Figures 6 and 7). That is why all the **PT1**, **PT2**, **PT3**, and

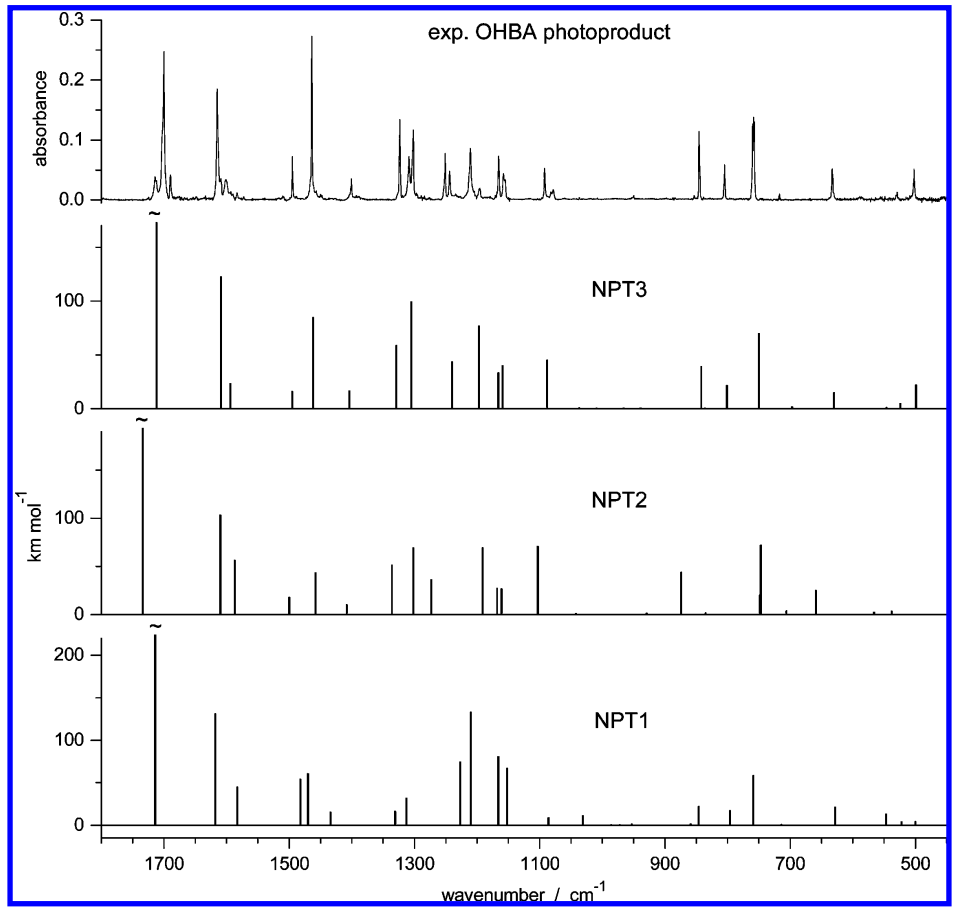

Figure 8. Comparison of the experimental IR spectrum of a photoproduct generated upon UV ($\lambda > 335$ nm) irradiation of OHBA with the spectra theoretically predicted for isomers **NPT3**, **NPT2**, and **NPT1** of the compound. The theoretical spectra were calculated at the DFT(B3LYP)/6-311++G(2d,p) level. Theoretical wavenumbers were scaled by 0.98.

OXET structures can be safely ruled out as plausible candidates for the isomers photogenerated from OHBA and OHAP.

The infrared spectra predicted for **NPT1**, **NPT2**, and **NPT3** structures of OHBA and OHAP are juxtaposed in Figures 8 and 9 with the experimental spectra of products generated upon UV irradiation of the compounds. As evident from the comparison of the spectra presented in these figures, an excellent agreement between the experiment and the theoretical simulation was found only in the case of the spectra calculated for **NPT3** isomers with OH and formyl (or acetyl) groups rotated each by 180°. For both studied compounds, one can easily observe a nearly perfect one-to-one correspondence between the IR bands of the experimental spectra and those of the calculated spectrum of **NPT3**. Good agreement concerns not only the band positions in theoretical and experimental spectra but also the pattern of relative intensities. In the case of the spectra predicted for **NPT1** and **NPT2** isomers the discrepancies with the experimental results are easily noticeable in Figures 8 and 9. Hence, the structures **NPT3** can be reliably assigned to the UV-generated isomers of OHBA as well as of OHAP.

Other Phototransformations Occurring upon UV Irradiation of OHBA and OHAP. Irradiation of OHBA and OHAP, isolated in solid Ar at 12 K, with continuous-wave UV light emitted by high-pressure mercury or xenon−mercury lamps generates the non-hydrogen-bonded **NPT3** isomers as nearly the sole products stable in low-temperature matrix environment. Only minor indications of UV-induced transformations of the compounds to other species were observed. The spectral signatures of these photoproducts were observed at 2136, 2119 cm^{-1} (OHBA) and 2136, 2110 cm^{-1} (OHAP). Much more pronounced generation of these species occurred upon exposure of matrix-isolated OHBA to the pulsed (10 ns, 10 Hz) light (250 nm) of the frequency-doubled signal beam of a MOPO laser. Both **HB** and **NPT3** forms of OHBA were consumed during such irradiation and a significant quantity of the product absorbing at 2136 cm^{-1} was generated (see Figure 10). The high intensity and the characteristic spectral position of this emerging band suggest that the photoproduct has a ketene group in its structure.[32]

Conclusions

UV-induced isomerizations were observed for *o*-hydroxybenzaldehyde (OHBA) and *o*-hydroxyacetophenone (OHAP) monomers isolated in low-temperature Ar matrixes. Upon irradiation with UV ($\lambda > 335$ nm) light, these species were found to convert into non-hydrogen-bonded isomers. The most spectacular indication of these transformations is the appearance of the band at 3632 cm^{-1} (OHBA) and the band at 3625 cm^{-1} (OHAP) in the IR spectra recorded after UV irradiation. Such frequencies are characteristic of stretching vibrations of OH groups not involved in hydrogen bonding. Contrary to the previous reports,[15,16,20] the photoisomerization of OHAP isolated in solid Ar did not require (under the applied experimental conditions) any extraordinary long irradiation time. Subsequent irradiation with shorter-wavelength UV ($\lambda > 235$ nm or $\lambda > 270$ nm) light induced a partial repopulation of the initial forms (with intramolecular hydrogen bonding), for both OHBA and OHAP. This demonstrates that the photoequilibrium between the photoproduct and the substrate depends on the wavelength of UV light applied for irradiation.

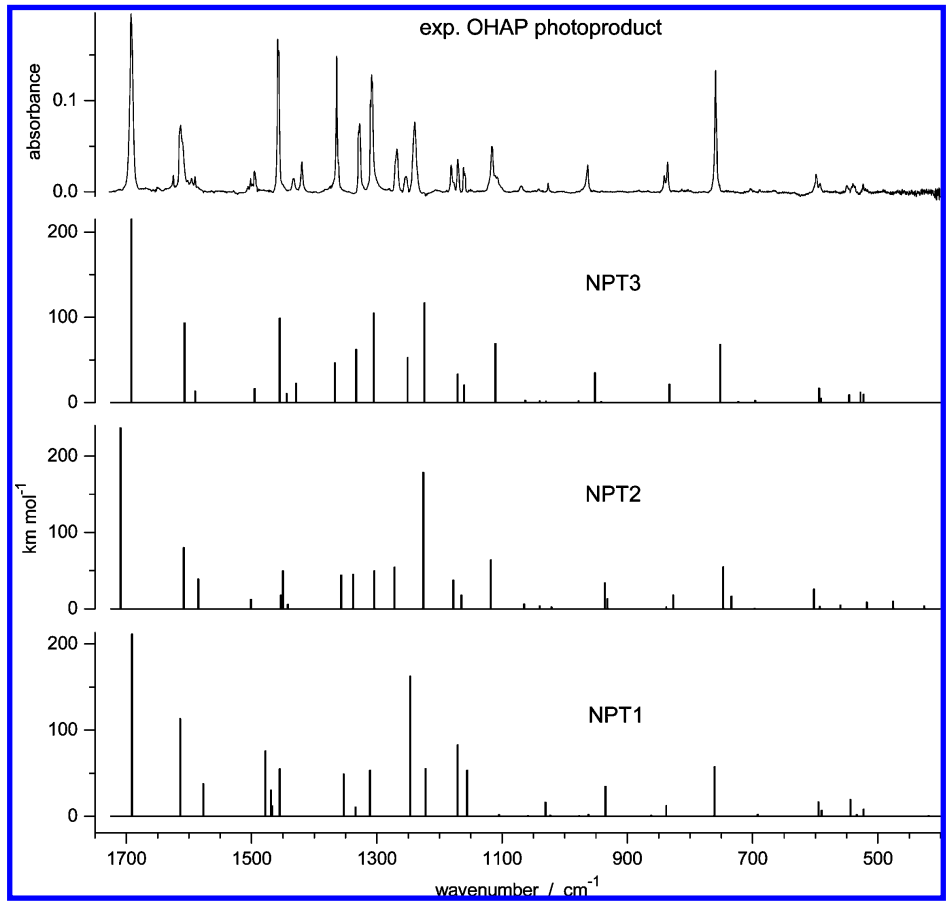

Figure 9. Comparison of the experimental IR spectrum of a photoproduct generated upon UV ($\lambda > 335$ nm) irradiation of OHAP with the spectra theoretically predicted for isomers **NPT3**, **NPT2**, and **NPT1** of the compound. The theoretical spectra were calculated at the DFT(B3LYP)/6-311++G(2d,p) level. Theoretical wavenumbers were scaled by 0.98.

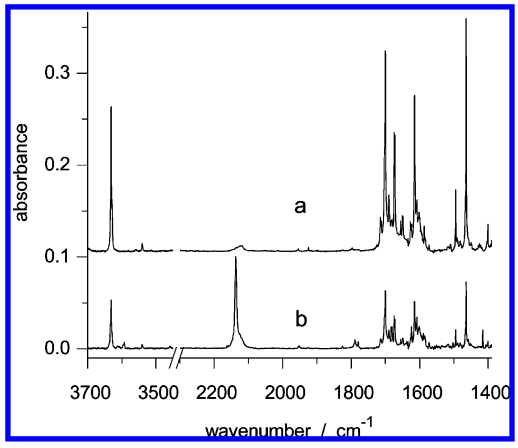

Figure 10. Infrared spectrum of OHBA monomers isolated in an Ar matrix (12 K): (a) after 30 min of UV irradiation with continuous-wave, filtered $\lambda > 235$ nm light of high-pressure Xe/Hg lamp; (b) after subsequent 2 h of irradiation with UV $\lambda = 250$ nm light generated in the frequency doubling module of the Quanta-Ray MOPO-SL optical parametric oscillator (repetition rate 10 Hz, pulse energy ~1 mJ) pumped with a pulsed (10 ns) Nd:YAG laser.

SCHEME 1: Photoisomerization Reactions Observed for OHBA and OHAP

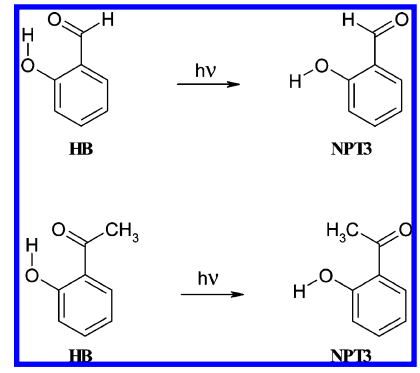

The photoproducts stabilized at 12 K in solid argon were characterized by FTIR spectroscopy. The experimental IR spectra of the products generated upon UV ($\lambda > 335$ nm) irradiation were compared with the spectra theoretically predicted for all possible candidate structures of non-hydrogen-bonded isomers. Excellent agreement with the experimental spectra was obtained (for OHBA as well as for OHAP) only in the case of theoretical spectra calculated for **NPT3** structure, with the OH group as well as the formyl (OHBA) or acetyl (OHAP) groups rotated each by 180° (see Scheme 1). This allowed a very reliable identification of the structure of photogenerated non-hydrogen-bonded isomers of *o*-hydroxybenzaldehyde and of *o*-hydroxyacetophenone. Such a straightforward and convincing evidence of the correctness of the assignment of **NPT3** structure to the photoisomers of OHBA and OHAP resolves the controversy over this issue that has been the subject of the long-lasting debate.

Acknowledgment. This work was partially supported by the Portuguese Science Foundation (FCT).

Supporting Information Available: Table S1 providing definitions of the internal coordinates used in the normal-mode

analysis carried out for the isomers of OHBA and OHAP. Tables S2 and S3 providing the assignment of the IR bands observed in the spectra of OHBA and OHAP isolated in Ar matrixes to the theoretical normal modes calculated [at the DFT(B3LYP)/6-311++G(2d,p) level] for the hydrogen-bonded isomers of these compounds. Tables S4 and S5 providing the assignment of the IR bands observed in the spectra of photoproducts generated upon UV irradiation of OHBA and OHAP isolated in Ar matrixes to the theoretical normal modes calculated [at the DFT(B3LYP)/6-311++G(2d,p) level] for the **NPT3** non-hydrogen-bonded isomers of these compounds. Tables S6 and S7 providing relative energies of OHBA and OHAP isomers calculated at the DFT(B3LYP)/6-311++G(2d,p) level. Figure S1 showing the theoretically calculated barrier separating **NPT1** and **NPT3** isomers of OHAP. This material is available free of charge via the Internet at http://pubs.acs.org.

References and Notes

(1) Weller, A. *Z. Elektrochem.* **1956**, *60*, 1144.
(2) Weller, A. *Prog. React. Kinet.* **1961**, *1*, 187.
(3) Formosinho, S. J.; Arnaut, L. G. *J. Photochem. Photobiol. A* **1993**, *75*, 21.
(4) Lochbrunner, S.; Schultz, T.; Schmitt, M.; Shaffer, J. P.; Zgierski, M. Z.; Stolow, A. *J. Chem. Phys.* **2001**, *114*, 2519.
(5) Stock, K.; Bizjak, T.; Lochbrunner, S. *Chem. Phys. Lett.* **2002**, *354*, 409.
(6) Douhal, A.; Lahmani, F.; Zewail, A. H. *Chem. Phys.* **1996**, *207*, 477.
(7) Herek, J. L.; Pedersen, S.; Banares, L.; Zewail, A. H. *J. Chem. Phys.* **1992**, *97*, 9046.
(8) Otterstedt, J. E. A.; Rater, R. *J. Heterocycl. Chem.* **1972**, *9*, 225.
(9) Otterstedt, J. E. A. *J. Chem. Phys.* **1973**, *58*, 5716.
(10) Heller, H. J.; Blattmann, H. R. *Pure Appl. Chem.* **1973**, *36*, 141.
(11) Chou, P. T.; McMorrow, D.; Aartsma, T. J.; Kasha, M. *J. Phys. Chem.* **1984**, *88*, 4596.
(12) Khan, A. U.; Kasha, M. *Proc. Natl. Acad. Sci. U.S.A.* **1983**, *80*, 1767.
(13) Acuna, A. U.; Amat-Guerri, F.; Catalan, J.; Costella, A.; Figuera, J. M.; Munoz, J. *Chem. Phys. Lett.* **1986**, *132*, 567.
(14) Munn, R. W. *Chem. Br.* **1989**, 517.
(15) Gebicki, J.; Krantz, A. *J. Chem. Soc., Perkin Trans.2* **1984**, 1617.
(16) Morgan, M. A.; Orton, E.; Pimentel, G. O. *J. Phys. Chem.* **1990**, *94*, 7927.
(17) Migani, A.; Blancafort, L.; Robb, M. A.; DeBellis, A. D. *J. Am. Chem. Soc.* **2008**, *130*, 6932.
(18) Lapinski, L.; Nowak, M. J.; Nowacki, J.; Rode, M. F.; Sobolewski, A. L. *ChemPhysChem* **2009**, *10*, 2290.
(19) Sobolewski, A. L.; Domcke, W. *Phys. Chem. Chem. Phys.* **2006**, *8*, 3410.
(20) Orton, E.; Morgan, M. A.; E.; Pimentel, G. O. *J. Phys. Chem.* **1990**, *94*, 7936.
(21) Becke, A. D. *Phys. Rev. A* **1988**, *38*, 3098.
(22) Lee, C. T.; Yang, W. T.; Parr, R. G. *Phys. Rev. B* **1988**, *37*, 785.
(23) Frisch, M. J.; Trucks, G. W.; Schlegel, H. B.; Scuseria, G. E.; Robb, M. A.; Cheeseman, J. R.; Montgomery, J. A., Jr.; Vreven, T.; Kudin, K. N.; Burant, J. C.; Millam, J. M.; Iyengar, S. S.; Tomasi, J.; Barone, V.; Mennucci, B.; Cossi, M.; Scalmani, G.; Rega, N.; Petersson, G. A.; Nakatsuji, H.; Hada, M.; Ehara, M.; Toyota, K.; Fukuda, R.; Hasegawa, J.; Ishida, M.; Nakajima, T.; Honda, Y.; Kitao, O.; Nakai, H.; Klene, M.; Li, X.; Knox, J. E.; Hratchian, H. P.; Cross, J. B.; Bakken, V.; Adamo, C.; Jaramillo, J.; Gomperts, R.; Stratmann, R. E.; Yazyev, O.; Austin, A. J.; Cammi, R.; Pomelli, C.; Ochterski, J. W.; Ayala, P. Y.; Morokuma, K.; Voth, G. A.; Salvador, P.; Dannenberg, J. J.; Zakrzewski, V. G.; Dapprich, S.; Daniels, A. D.; Strain, M. C.; Farkas, O.; Malick, D. K.; Rabuck, A. D.; Raghavachari, K.; Foresman, J. B.; Ortiz, J. V.; Cui, Q.; Baboul, A. G.; Clifford, S.; Cioslowski, J.; Stefanov, B. B.; Liu, G.; Liashenko, A.; Piskorz, P.; Komaromi, I.; Martin, R. L.; Fox, D. J.; Keith, T.; Al-Laham, M. A.; Peng, C. Y.; Nanayakkara, A.; Challacombe, M.; Gill, P. M. W.; Johnson, B.; Chen, W.; Wong, M. W.; Gonzalez, C.; Pople, J. A. *Gaussian 03, revision C.02*; Gaussian, Inc.: Wallingford, CT, 2004.
(24) Keresztury, G.; Jalsovszky, G. *J. Mol. Struct.* **1971**, *10*, 304.
(25) Rostkowska, H.; Lapinski, L.; Nowak, M. J. *Vibr. Spectrosc.* **2009**, *49*, 43.
(26) Pulay, P.; Fogarasi, G.; Pang, F.; Boggs, J. E. *J. Am. Chem. Soc.* **1979**, *101*, 2550.
(27) Rozenberg, M.; Shoham, G.; Reva, I.; Fausto, R. *Phys. Chem. Chem. Phys.* **2005**, *7*, 2376.
(28) Plokhotnichenko, A. M.; Radchenko, E. D.; Blagoi, Yu., P.; Karachevtsev, V. A. *Low Temp. Phys.* **2001**, *27*, 666.
(29) Bist, H. D.; Brand, J. C. D.; Williams, D. R. *J. Mol. Spectrosc.* **1967**, *24*, 402.
(30) Coleman, W. M.; Gordon, B. M. *Appl. Spectrosc.* **1987**, *41*, 1169.
(31) Coleman, W. M.; Gordon, B. M. *Appl. Spectrosc.* **1988**, *42*, 304.
(32) Breda, S.; Reva, I.; Lapinski, L.; Fausto, R. *Phys. Chem. Chem. Phys.* **2004**, *6*, 929.

JP1003775